2-1-1984

Laminar Condensation on a Moving Drop. Part 1. Singular Perturbation Technique

J. N. Chung
Washington State University

Portonovo S. Ayyaswamy
University of Pennsylvania, ayya@seas.upenn.edu

Satwindar S. Sadhal
University of Southern California

Laminar Condensation on a Moving Drop. Part 1. Singular Perturbation Technique

Abstract

In this paper, laminar condensation on a spherical drop in a forced flow is investigated. The drop experiences a strong, radial, condensation-induced velocity while undergoing slow translation. In view of the high condensation velocity, the flow field, although the drop experiences slow translation, is not in the Stokes-flow regime. The drop environment is assumed to consist of a mixture of saturated steam (condensable) and air (non-condensable). The study has been carried out in two different ways. In Part 1 the continuous phase is treated as quasi-steady and the governing equations for this phase are solved through a singular perturbation technique. The transient heat-up of the drop interior is solved by the series-truncation numerical method. The solution for the total problem is obtained by matching the results for the continuous and dispersed phases. I n Part 2 both the phases are treated as fully transient and the entire set of coupled equations are solved by numerical means. Validity of the quasi-steady assumption of Part 1 is discussed. Effects due to the presence of the non-condensable component and of the drop surface temperature on transport processes are discussed in both parts. A significant contribution of the present study is the inclusion of the roles played by both the viscous and the inertial effects in the problem treatment.

Disciplines
Engineering | Mechanical Engineering

Laminar condensation on a moving drop. Part 1. Singular perturbation technique

By J. N. CHUNG,

Department of Mechanical Engineering, Washington State University,
Pullman, WA 99164–2920

P. S. AYYASWAMY

Department of Mechanical Engineering and Applied Mechanics, University of Pennsylvania,
Philadelphia, PA 19104

AND S. S. SADHAL

Department of Mechanical Engineering, University of Southern California,
Los Angeles, CA 90089–1453

In this paper, laminar condensation on a spherical drop in a forced flow is investigated. The drop experiences a strong, radial, condensation-induced velocity while undergoing slow translation. In view of the high condensation velocity, the flow field, although the drop experiences slow translation, is not in the Stokes-flow regime. The drop environment is assumed to consist of a mixture of saturated steam (condensable) and air (non-condensable). The study has been carried out in two different ways. In Part 1 the continuous phase is treated as quasi-steady and the governing equations for this phase are solved through a singular perturbation technique. The transient heat-up of the drop interior is solved by the series-truncation numerical method. The solution for the total problem is obtained by matching the results for the continuous and dispersed phases. In Part 2 both the phases are treated as fully transient and the entire set of coupled equations are solved by numerical means. Validity of the quasi-steady assumption of Part 1 is discussed. Effects due to the presence of the non-condensable component and of the drop surface temperature on transport processes are discussed in both parts. A significant contribution of the present study is the inclusion of the roles played by both the viscous and the inertial effects in the problem treatment.

1. Introduction

In Parts 1 and 2 of the present study we investigate the hydrodynamics and heat/mass transfer associated with laminar condensation on a water drop translating in a mixture of saturated steam (condensable) and air (non-condensable). The effect of translation itself is brought into focus through its introduction as a perturbation to an otherwise stationary drop experiencing condensation. There are many studies in published literature that deal with a variety of situations involving the heat and mass transfer and/or the hydrodynamic aspects of drop motion (Clift, Grace & Weber 1978). However, there are very few comprehensive studies of laminar condensation on a liquid drop translating in its own vapour along with a non-condensable (see e.g. Chung & Ayyaswamy 1981*a*, *b*). In particular, the effect of a strong normal velocity,
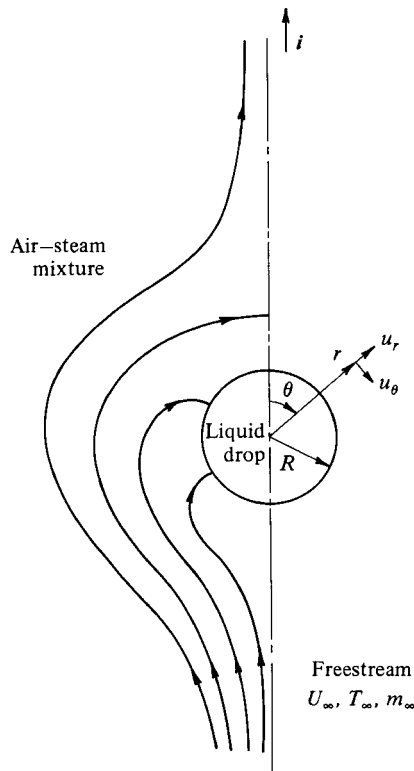
FIGURE 1. Geometry and coordinate system.

induced by condensation, on the convective transport together with slow translation has not been investigated. This situation arises in many practical/industrial applications and is also of interest to atmospheric science. Here, we have examined such heat/mass transport effects in detail. Several novel features are revealed and these will be discussed subsequently.

The analysis is carried out in two different ways. In this paper we approximate the continuous phase as quasi-steady while the dispersed phase is unsteady. We justify this approximation by examining the magnitudes of the thermal and mass diffusivities in the gas–vapour phase and comparing them with the thermal diffusivity in the liquid phase. The former are much higher than the latter. The liquid thermal diffusivity therefore controls the drop heat-up time. On this timescale the transients in the gas–vapour phase die out much faster. The quasi-steady nature of the continuous phase admits an asymptotic approach. The corresponding energy and species equations for this phase are solved through a singular matched-asymptotic technique. The equations are expanded in terms of small parameters and Legendre functions and solved up to first-order accuracy through inner and outer matching. The transient heat-up of the drop interior is solved by the series-truncation method and is carefully matched at the interface with the continuous phase solution.

In Part 2 (Chung, Ayyaswamy & Sadhal 1984) both the phases are treated as fully transient and the entire set of coupled equations is solved numerically. The relevant details of the numerical scheme have been provided. The validity of the quasi-steady approximation for the continuous phase made in the present paper is then discussed along with the results of sample calculations.

2. Theoretical formulation

Consider a liquid drop of radius R translating at a constant velocity U_∞, with a fully developed internal motion, in a large content of an otherwise quiescent binary mixture of its own vapour (condensable) and a gas (non-condensable). The drop is initially cold at a temperature T_0, while the binary mixture is saturated at a temperature T_∞ ($T_\infty > T_0$). The mass fraction m_∞ for the gas component is taken to be prescribed. We associate with the motion of the drop a 'translational Reynolds number' $Re_\infty = U_\infty R/\nu_\infty$, where ν_∞ is the kinematic viscosity of the mixture. In this paper we investigate situations for which $Re_\infty = \epsilon \ll 1$, while the Reynolds number Re_c associated with the normal velocity due to condensation at the interface is of order unity. We set $Re_c = U_{c\,max} R/\nu_\infty$, where $U_{c\,max}$ is the maximum of the normal velocity U_c at the interface. The subscript ∞ refers to properties evaluated at the freestream.

It is important to note that the complete flow field in this problem is not Stokes flow. There is a transfer of momentum from the mainstream towards the drop through the inertial terms associated with the prevailing radial field. In this analysis it is implicitly assumed that the rate of change of the liquid drop volume due to condensation is small, even though the condensation-induced radial velocity may be large. The effect of the variation in the drop radius is therefore considered to be negligible. This assumption is based on the large ratio of the liquid to the gas phase densities. The rate of change of the drop radius is of the order

$$\dot{R} = U_c \frac{\rho_\infty}{\rho_\ell},$$

where ρ_∞ and ρ_ℓ are the densities in the continuous and the dispersed phases respectively. The timescale governing substantial change in drop size is therefore

$$t_{\dot{R}} = \frac{R}{\dot{R}} = \frac{\rho_\ell}{\rho_\infty} \frac{R}{U_c}.$$

On the other hand, in the continuous phase the timescale governing the viscous diffusion is $t_\nu = R^2/\nu_\infty$, where ν_∞ is the kinematic viscosity. In order that we may neglect the effects of change in drop size, it is required that $t_\nu \ll t_{\dot{R}}$, or

$$\frac{t_\nu}{t_{\dot{R}}} = \frac{U_c R \rho_\infty}{\nu_\infty \rho_\ell} \ll 1.$$

In the present study $\rho_\infty/\rho_\ell = O(10^{-3})$ and $U_c R/\nu_\infty$ may be as large as 10. It follows that

$$\frac{t_\nu}{t_{\dot{R}}} = O(10^{-2}).$$

It is therefore justified to neglect the transient effects of the change in the drop size on the drop motion. By entirely similar arguments the heat and mass diffusion transients in the continuous phase may be neglected.

For the range of parameters considered in this paper, noting that the liquid drop has a large surface tension, the effect of any deviation from sphericity on the heat and mass transport is likely to be negligible.

2.1. *Quasi-steady condensation in the continuous phase*

We shall assume the physical properties to be constant and the Prandtl number $(Pr = \nu_\infty/\alpha_\infty)$ and the Schmidt number $(Sc = \nu_\infty/D_{12\infty})$ of the continuous phase to be of order unity. Here α_∞ is the thermal diffusivity and $D_{12\infty}$ is the binary diffusion coefficient of the ambient mixture. We impose the restriction that $|T_\infty - T_O|/T_\infty \ll 1$ and consequently neglect any free convective effects.

With these approximations we may write the governing equations. For the continuous phase we have

$$\boldsymbol{\nabla}\cdot\boldsymbol{u} = 0, \tag{1 a}$$

$$\boldsymbol{u}\cdot\boldsymbol{\nabla}\boldsymbol{u} + \frac{1}{\rho_\infty}\boldsymbol{\nabla}p = \nu_\infty\nabla^2\boldsymbol{u}, \tag{1 b}$$

$$\frac{1}{\alpha_\infty}(\boldsymbol{u}\cdot\boldsymbol{\nabla}T) = \nabla^2 T, \tag{1 c}$$

$$\frac{1}{D_{12\infty}}(\boldsymbol{u}\cdot\boldsymbol{\nabla}m) = \nabla^2 m, \tag{1 d}$$

where $\boldsymbol{u}$ is the velocity, T is the temperature, m is the noncondensable mass fraction, p is the pressure and ρ_∞ is the density.

It would be convenient to make the above equations dimensionless. First, we need to choose proper scaling parameters for the velocity. Following Sadhal & Ayyaswamy (1983), consider writing

$$\boldsymbol{u} = \boldsymbol{u}_0 + \boldsymbol{u}', \tag{2}$$

where $\boldsymbol{u}_0$ is the purely radial field that would be present in the absence of any translation. The quantity $\boldsymbol{u}'$ represents the change in the flow field due to translation at a velocity U_∞. Clearly $\boldsymbol{u}'$ has a radial component which will enhance the condensation-induced flow field. With A_0 denoting the radial velocity at the interface in the absence of translation, we may write

$$\boldsymbol{u}_0 = A_0\frac{R^2}{r^2}\hat{\boldsymbol{r}}, \tag{3}$$

where $\hat{\boldsymbol{r}}$ is the unit vector normal to the drop surface. In general, A_0 is an unknown governed by the thermodynamics of the stationary problem. We note that U_c defined earlier is of the same order as A_0, and, in fact, coincides with A_0 in the absence of translation. Now we define

$$\boldsymbol{u}^* = \frac{\boldsymbol{u}R}{\nu_\infty}, \quad \boldsymbol{u}_0^* = \frac{\boldsymbol{u}_0}{A_0}, \quad \boldsymbol{u}'^* = \frac{\boldsymbol{u}'}{U_\infty}, \quad A_{00} = \frac{A_0 R}{\nu_\infty}. \tag{4}$$

From (2) and (4)

$$\boldsymbol{u}^* = A_{00}\boldsymbol{u}_0^* + \epsilon\boldsymbol{u}'^*. \tag{5}$$

The dimensionless velocity collapses to purely radial flow as the translatory parameter ϵ vanishes. Similarly the pressure may be separated as $p = p_0 + p'$, which may be written in dimensionless form as

$$p^* = A_{00}p_0^* + \epsilon p'^*, \tag{6}$$

where

$$p'^* = \frac{p'}{\mu_\infty U_\infty/R}, \quad p_0^* = \frac{p_0}{\mu_\infty A_0/R}, \quad p^* = \frac{pR^2}{\mu_\infty\nu_\infty}.$$

The other non-dimensional quantities are defined as follows:

$$T^* = \frac{T - T_\infty}{T_0 - T_\infty}, \quad w^* = m - m_\infty, \quad r^* = \frac{r}{R}, \quad \boldsymbol{\nabla}^* = R\boldsymbol{\nabla}.$$

With omission of asterisks, the set of equations (1) in dimensionless form become

$$\boldsymbol{\nabla}\cdot\boldsymbol{u}' = 0, \tag{7a}$$

$$A_{00}(\boldsymbol{u}'\cdot\boldsymbol{\nabla}\boldsymbol{u}_0 + \boldsymbol{u}_0\cdot\boldsymbol{\nabla}\boldsymbol{u}') + \epsilon(\boldsymbol{u}'\cdot\boldsymbol{\nabla}\boldsymbol{u}') + \boldsymbol{\nabla}p' = \nabla^2\boldsymbol{u}', \tag{7b}$$

$$Pr(A_{00}\boldsymbol{u}_0 + \epsilon\boldsymbol{u}')\cdot\boldsymbol{\nabla}T = \nabla^2 T, \tag{7c}$$

$$Sc(A_{00}\boldsymbol{u}_0 + \epsilon\boldsymbol{u}')\cdot\boldsymbol{\nabla}w = \nabla^2 w. \tag{7d}$$

For the liquid phase let

$$\boldsymbol{u}_\ell = \boldsymbol{u}_{\ell 0} + \boldsymbol{u}'_\ell = \boldsymbol{u}'_\ell, \tag{8a}$$

$$p_\ell = p_{\ell 0} + p'_\ell, \tag{8b}$$

where the subscript zero refers to quantities in the absence of translation. Clearly $u_{\ell 0}$ must be zero. Scale

$$\boldsymbol{u}^*_\ell = \frac{\boldsymbol{u}_\ell R}{\nu_\ell}, \quad \boldsymbol{u}'^*_\ell = \frac{\boldsymbol{u}'_\ell}{U_\infty}, \quad p^*_{\ell 0} = \frac{p_{\ell 0}}{A_0 \mu_\ell/R}, \quad p'^*_\ell = \frac{p'_\ell}{\mu_\ell U_\infty/R}, \quad p^*_\ell = \frac{p_\ell R^2}{\mu_\ell \nu_\ell},$$

and introduce $Re_\ell = U_\infty R/\nu_\ell$ to obtain

$$\boldsymbol{u}^*_\ell = Re_\ell \boldsymbol{u}'^*_\ell, \tag{9a}$$

$$p^*_\ell = \phi_\nu A_{00} p^*_{\ell 0} + Re_\ell p'^*_\ell, \tag{9b}$$

where $\phi_\nu = \nu_\infty/\nu_\ell$. Let the dimensionless time $t^* = t\alpha_\ell/R^2$. Noting that $\boldsymbol{\nabla}p_{\ell 0} = 0$, and omitting the asterisks, the governing equations for the liquid side may be written as

$$\boldsymbol{\nabla}\cdot\boldsymbol{u}'_\ell = 0, \tag{10a}$$

$$\epsilon\phi_\nu(\boldsymbol{u}'_\ell\cdot\boldsymbol{\nabla}\boldsymbol{u}'_\ell) + \boldsymbol{\nabla}p'_\ell = \nabla^2\boldsymbol{u}'_\ell, \tag{10b}$$

$$\frac{\partial T_\ell}{\partial t} + Re_\ell Pr_\ell(\boldsymbol{u}'_\ell\cdot\boldsymbol{\nabla}T_\ell) = \nabla^2 T_\ell, \tag{10c}$$

where $Pr_\ell = \nu_\ell/\alpha_\ell$.

The initial and boundary conditions are as follows:

initial condition
$$T_\ell = 1 \quad (t = 0); \tag{11}$$

far-field conditions
$$T \to 0, \quad w \to 0, \quad \boldsymbol{u} \to \epsilon\boldsymbol{i} \quad \text{as} \quad r \to \infty, \tag{12}$$

where $\boldsymbol{i}$ is a unit vector in the direction of the uniform stream;

interface conditions
$$(A_{00}\boldsymbol{u}_0 + \epsilon\boldsymbol{u}')\cdot\boldsymbol{t} = \epsilon\boldsymbol{u}'_\ell\cdot\boldsymbol{t}, \tag{13a}$$

$$\phi_\nu \boldsymbol{\tau}(\boldsymbol{n})\cdot\boldsymbol{t} = \boldsymbol{\tau}_\ell(\boldsymbol{n})\cdot\boldsymbol{t}, \tag{13b}$$

$$T = T_\ell, \tag{13c}$$

$$(A_{00}\boldsymbol{u}_0 + \epsilon\boldsymbol{u}')\cdot\boldsymbol{n} = \frac{1}{m_i Sc}(\boldsymbol{\nabla}w)\cdot\boldsymbol{n}, \tag{13d}$$

$$\phi_k\left[-\frac{Pr}{Ja}(A_{00}\boldsymbol{u}_0 + \epsilon\boldsymbol{u}') + \boldsymbol{\nabla}T\right]\cdot\boldsymbol{n} = \boldsymbol{\nabla}T_\ell\cdot\boldsymbol{n} \tag{13e}$$

$(r = 1),$

where m_i is the non-condensable mass fraction at the interface, τ is the dimensionless stress tensor, $Ja = c_{p\infty}\,\Delta T/\lambda$ is the Jakob number, $\phi_k = k_\infty/k_\ell$, $\Delta T = T_0 - T_\infty$, λ is the latent heat of evaporation, and t and n refer to the unit tangential and unit normal vectors respectively. Equation (13d) represents the condition of impermeability of the non-condensable component, and (13e) is the interfacial heat balance.

2.2. *Perturbation expansions, governing equations and velocity field solutions*

Letting $u' = u_1 + \epsilon u_2 + O(\epsilon^2)$, and using (5), with the asterisks omitted, we have

$$u = A_{00}\,u_0 + \epsilon u_1 + O(\epsilon^2). \tag{14}$$

The total normal velocity at the interface may be perturbed as

$$u \cdot n = A_{00} + \epsilon u' \cdot n = A_{00} + \epsilon A_1(\theta) + O(\epsilon^2), \tag{15}$$

where $\epsilon A_1(\theta)$ represents an increase in the condensation-induced velocity resulting from translation. The other variables may be similarly perturbed as

$$\left.\begin{aligned}
\epsilon u'_\ell &= \epsilon u_{\ell 1} + O(\epsilon^2), \quad \tau = \tau_0 + \epsilon\tau_1 + O(\epsilon^2), \\
\tau_\ell &= \tau_{\ell 0} + \epsilon\tau_{\ell 1} + O(\epsilon^2), \quad T = \hat{T}_0 + \epsilon\hat{T}_1 + O(\epsilon^2), \\
T_\ell &= T_{\ell 0} + \epsilon T_{\ell 1} + O(\epsilon^2), \quad w = w_0 + \epsilon w_1 + O(\epsilon^2), \\
\epsilon p' &= \epsilon p_1 + O(\epsilon^2), \quad \epsilon p'_\ell = \epsilon p_{\ell 1} + O(\epsilon^2), \\
m_i &= m_{i0} + \epsilon m_{i1} + O(\epsilon^2).
\end{aligned}\right\} \tag{16}$$

The equations for the flow field for order ϵ^1 are

$$\nabla \cdot u_1 = 0, \tag{17a}$$

$$A_{00}(u_1 \cdot \nabla u_0 + u_0 \cdot \nabla u_1) + \nabla p_1 = \nabla^2 u_1, \tag{17b}$$

$$\nabla \cdot u_{\ell 1} = 0, \tag{17c}$$

$$\nabla p_{\ell 1} = \nabla^2 u_{\ell 1}. \tag{17d}$$

The boundary conditions are

$$u_1 = i \quad \text{as} \quad r \to \infty, \tag{18}$$

$$\left.\begin{aligned}
u_1 \cdot t &= u_{\ell 1} \cdot t, \\
\tau_1(n) \cdot t &= \tau_{\ell 1}(n) \cdot t, \\
u_1 \cdot n &= A_1(\theta)
\end{aligned}\right\} \quad (r = 1). \tag{19}$$

In general $A_1(\theta)$ is an arbitrary function of θ governed partly by the thermodynamics. It is possible to expand it as an infinite series of Legendre polynomials: $A_1(\theta) = \sum_{n=0}^{\infty} A_{1n} P_n(\cos\theta)$. However, a detailed analysis has revealed that, up to order ϵ, $A_1(\theta)$ assumes the same characteristics as the variable causing the perturbation, namely the translational field. Hence, in view of (18) (i.e. $u_{1r}|_{r\to\infty} = \cos\theta$), we keep terms only up to $P_1(\cos\theta)$, and let

$$A_1(\theta) = A_{01} + A_{11}\cos\theta. \tag{20}$$

Subsequent inner and outer matching of the thermodynamic variables will indeed show the sufficient generality, in the formulation up to $O(\epsilon)$, of the representation given in (20).

In a different context, Sadhal & Ayyaswamy (1983) have solved the set of equations

(17 *a–d*) subject to boundary conditions (18) and (19) in spherical coordinates. Their results, in component form, are

$$u_{1r} = \frac{A_{01}}{r^2} + \left\{ 1 + \frac{B}{r^3} + \frac{C}{r^2} \left[\frac{A_{00}}{r} \int_{1/A_{00}}^{r/A_{00}} (\xi^4 + \xi^3)\, e^{-1/\xi}\, d\xi - \frac{1}{5}\left(\frac{r}{A_{00}}\right)^4 + \frac{1}{6}\left(\frac{r}{A_{00}}\right)^2 \right] \right\} \cos\theta, \tag{21}$$

$$u_{1\theta} = -\frac{1}{2}\left\{ 2 - \frac{B}{r^3} + \frac{C}{r^2}\left[-\frac{A_{00}}{r}\int_{1/A_{00}}^{r/A_{00}} (\xi^4 + \xi^3)\, e^{-1/\xi}\, d\xi \right. \right.$$

$$\left. \left. + \left[\left(\frac{r}{A_{00}}\right)^4 + \left(\frac{r}{A_{00}}\right)^3\right] e^{-A_{00}/r} - \frac{4}{5}\left(\frac{r}{A_{00}}\right)^4 + \frac{1}{3}\left(\frac{r}{A_{00}}\right)^2 \right] \right\} \sin\theta, \tag{22}$$

$$u_{\ell 1r} = \hat{B}(r^2 - 1)\cos\theta, \tag{23}$$

$$u_{\ell 1\theta} = -\hat{B}(2r^2 - 1)\sin\theta, \tag{24}$$

where

$$B = -(1 - A_{11}) + [(3 + 2\phi_\mu) - (1 + 2\phi_\mu)A_{11}](-\tfrac{1}{5} + \tfrac{1}{6}A_{00}^2)/G, \tag{25}$$

$$C = -[(3 + 2\phi_\mu) - (1 + 2\phi_\mu)A_{11}]A_{00}^4/G, \tag{26}$$

$$\hat{B} = \phi_\mu\{(1 - A_{11})[1 - \tfrac{1}{3}A_{00}^2 - (1 + A_{00} + \tfrac{1}{6}A_{00}^2)\, e^{-A_{00}}] + \tfrac{1}{3}A_{00}^2(1 - e^{-A_{00}})\}/G, \tag{27}$$

with
$$G = -1 + \tfrac{1}{6}(3 + 2\phi_\mu)A_{00}^2 + (1 + A_{00} - \tfrac{1}{3}\phi_\mu A_{00}^2)\, e^{-A_{00}} \tag{28}$$

and $\phi_\mu = \mu_\infty/\mu_\ell$. We note that the flow field in the liquid phase is a form of the Hill's spherical vortex and is an exact solution of the full Navier–Stokes momentum equations.

The energy and the species equations for the perturbed fields may be written as follows.

Leading order ϵ^0:

$$Pr\, A_{00}\, \boldsymbol{u}_0 \cdot \boldsymbol{\nabla}\hat{T}_0 = \nabla^2 \hat{T}_0, \tag{29a}$$

$$Sc\, A_{00}\, \boldsymbol{u}_0 \cdot \boldsymbol{\nabla}w_0 = \nabla^2 w_0, \tag{29b}$$

$$\frac{\partial T_{\ell 0}}{\partial t} = \nabla^2 T_{\ell 0}; \tag{29c}$$

with boundary conditions

$$\hat{T}_0 \to 0, \quad w_0 \to 0 \quad \text{as} \quad r \to \infty, \tag{30}$$

$$\hat{T}_0 = T_{\ell 0}, \tag{31a}$$

$$\phi_k\left[-\frac{Pr}{Ja}A_{00} + \boldsymbol{\nabla}\hat{T}_0 \cdot \boldsymbol{n} \right] = \boldsymbol{\nabla}T_{\ell 0} \cdot \boldsymbol{n}, \qquad (r = 1), \tag{31b}$$

$$A_{00} = \frac{1}{m_{i0}Sc}(\boldsymbol{\nabla}w_0 \cdot \boldsymbol{n}) \tag{31c}$$

and initial condition
$$T_{\ell 0} = 1 \quad (t = 0). \tag{32}$$

First order ϵ^1:

$$Pr(A_{00}\, \boldsymbol{u}_0 \cdot \boldsymbol{\nabla}\hat{T}_1 + \boldsymbol{u}_1 \cdot \boldsymbol{\nabla}\hat{T}_0) = \nabla^2 \hat{T}_1, \tag{33a}$$

$$Sc(A_{00}\, \boldsymbol{u}_0 \cdot \boldsymbol{\nabla}w_1 + \boldsymbol{u}_1 \cdot \boldsymbol{\nabla}w_0) = \nabla^2 w_1, \tag{33b}$$

$$\frac{\partial T_{\ell 1}}{\partial t} + \phi_\nu\, Pr_\ell(\boldsymbol{u}_{\ell 1} \cdot \boldsymbol{\nabla}T_{\ell 0}) = \nabla^2 T_{\ell 1}; \tag{33c}$$

with boundary conditions

$$\hat{T}_1 \to 0, \quad w_1 \to 0 \quad \text{as} \quad r \to \infty, \tag{34}$$

$$\hat{T}_1 = T_{\ell 1}, \tag{35a}$$

$$\phi_k \left[-\frac{Pr}{Ja} \mathbf{u}_1 + \nabla \hat{T}_1 \right] \cdot \mathbf{n} = \nabla T_{\ell 1} \cdot \mathbf{n}, \qquad \Bigg\} \quad (r = 1), \tag{35b}$$

$$[A_{00} m_{11} + (\mathbf{u}_1 \cdot \mathbf{n}) m_{i0}] = \frac{1}{Sc} \nabla w_1 \cdot \mathbf{n} \tag{35c}$$

and initial condition

$$T_{\ell 1} = 0 \quad (t = 0). \tag{36}$$

Before attempting to solve the above set of equations explicitly, we note that the velocity $\mathbf{u}_1$ which appears in (14) and (33a, b) is non-zero as $r \to \infty$ (uniform stream). In view of this, the non-homogeneous terms $\mathbf{u}_1 \cdot \nabla \hat{T}_0$ and $\mathbf{u}_1 \cdot \nabla w_0$ in (33a, b) lead to exact solutions for $\hat{T}_1$ and w_1 which cannot be made to satisfy the boundary conditions at infinity, as demanded by (34). This apparent difficulty is due to the existence of a region of non-uniformity in the neighbourhood of the point at infinity (see Acrivos & Taylor 1962). Therefore we invoke the singular perturbation procedure in which the leading-order description for the far-field temperature and mass fraction includes the perturbed velocity field. The details are given in §3.

3. Solution for the continuous phase by singular perturbation

The treatment of the problem by singular perturbation requires a reexamination of the unperturbed equations (7c, d). At this point it is convenient to write these in spherical coordinates, viz

$$\frac{1}{r^2} \frac{\partial}{\partial r} \left(r^2 \frac{\partial T}{\partial r} \right) + \frac{1}{r^2} \frac{\partial}{\partial \bar{\mu}} (1 - \bar{\mu}^2) \frac{\partial T}{\partial \bar{\mu}} = Pr \left[\left(\frac{A_{00}}{r^2} + \epsilon u_{1r} \right) \frac{\partial T}{\partial r} - \epsilon \frac{u_{1\theta}}{r} (1 - \bar{\mu}^2)^{\frac{1}{2}} \frac{\partial T}{\partial \bar{\mu}} \right], \tag{37}$$

$$\frac{1}{r^2} \frac{\partial}{\partial r} \left(r^2 \frac{\partial w}{\partial r} \right) + \frac{1}{r^2} \frac{\partial}{\partial \bar{\mu}} (1 - \bar{\mu}^2) \frac{\partial w}{\partial \bar{\mu}} = Sc \left[\left(\frac{A_{00}}{r^2} + \epsilon u_{1r} \right) \frac{\partial w}{\partial r} - \epsilon \frac{u_{1\theta}}{r} (1 - \bar{\mu}^2)^{\frac{1}{2}} \frac{\partial w}{\partial \bar{\mu}} \right], \tag{38}$$

where $\bar{\mu} = \cos \theta$. While the unperturbed equations are difficult to solve exactly, an asymptotic solution in the limit $r \to \infty$ is possible to obtain. This solution would give a meaningful description in the outer region. It is in this outer region that (33a, b) do not yield a uniformly valid solution. The singular perturbation procedure requires one to obtain an outer solution, valid for $r \to \infty$, and to match it with the solutions for (33a, b) which are valid in the inner region ($r \to 1$). As a result, uniformly valid solutions may be obtained for the entire domain. The outer asymptotic solution is obtained by defining a strained radial coordinate $\rho = \epsilon r$, and writing (7c, d) in terms of ρ. The leading-order description for small ϵ in this coordinate includes the perturbed velocity field and thus gives the proper asymptotic behaviour for T and w as $r \to \infty$. A formal treatment by this method requires one to employ a more general perturbation scheme than the one given in (16). The detailed procedure follows.

3.1. *Singular perturbation procedure*

We assume sufficiently general forms for the inner expansions to be

$$T(r, \bar{\mu}; \epsilon) = \sum_{n=0}^{\infty} f_n(\epsilon) t_n(r, \bar{\mu}) = \sum_{n=0}^{\infty} \sum_{m=0}^{\infty} f_n(\epsilon) l_{mn}(r) P_m(\bar{\mu}), f_0(\epsilon)$$

$$= 1, \tag{39}$$

$$w(r,\bar{\mu};\epsilon) = \sum_{n=0}^{\infty} \bar{f}_n(\epsilon)\, w_m(r,\bar{\mu}) = \sum_{n=0}^{\infty} \sum_{m=0}^{\infty} \bar{f}_n(\epsilon)\, \bar{l}_{mn}(r)\, P_m(\bar{\mu}), \bar{f}_0(\epsilon)$$
$$= 1. \tag{40}$$

The boundary conditions at the interface consist of matching of the continuous phase with the dispersed phase. First we shall assume arbitrary values imposed at the interface, viz

$$T(1,\bar{\mu};\epsilon) = T_{\mathrm{i}}(\bar{\mu};\epsilon), \tag{41}$$

$$w(1,\bar{\mu};\epsilon) = w_{\mathrm{i}}(\bar{\mu};\epsilon). \tag{42}$$

Owing to the structural similarity between the energy and the species equations, the techniques for the solution in each case are the same. We therefore provide the details only for the temperature solutions. However, the final solution for the species transport is given. We expand these boundary conditions in the same fashion as (39) and (40). Thus we write

$$T_{\mathrm{i}}(\bar{\mu};\epsilon) = \sum_{n=0}^{\infty} \sum_{m=0}^{\infty} f_n(\epsilon)\, t_{\mathrm{i}mn}\, P_m(\bar{\mu}), \tag{43}$$

$$w_{\mathrm{i}}(\bar{\mu};\epsilon) = \sum_{n=0}^{\infty} \sum_{m=0}^{\infty} \bar{f}_n(\epsilon)\, w_{\mathrm{i}mn}\, P_m(\bar{\mu}). \tag{44}$$

In the above, $P_m(\bar{\mu})$ denotes the Legendre polynomial of order m. The perturbation parameters $f_n(\epsilon)$ and $\bar{f}_n(\epsilon)$ are yet to be determined. The restrictions applicable are

$$\lim_{\epsilon \to 0} \frac{f_{n+1}(\epsilon)}{f_n(\epsilon)} = 0, \quad \lim_{\epsilon \to 0} \frac{\bar{f}_{n+1}(\epsilon)}{\bar{f}_n(\epsilon)} = 0.$$

Next we introduce $\rho = r\epsilon$ as a strained radial coordinate for the outer expansion and consider an outer expansion of the form

$$T(r,\bar{\mu};\epsilon) = \hat{T}(\rho,\bar{\mu},\epsilon) = \sum_{n=0}^{\infty} F_n(\epsilon)\, \hat{t}_n(\rho,\bar{\mu}), \tag{45}$$

$$w(r,\bar{\mu};\epsilon) = \hat{w}(\rho,\bar{\mu},\epsilon) = \sum_{n=0}^{\infty} \bar{F}_n(\epsilon)\, \hat{w}_n(\rho,\bar{\mu}), \tag{46}$$

with
$$\lim_{\epsilon \to 0} \frac{F_{n+1}(\epsilon)}{F_n(\epsilon)} = 0, \quad \lim_{\epsilon \to 0} \frac{\bar{F}_{n+1}(\epsilon)}{\bar{F}_n(\epsilon)} = 0.$$

3.2. *Lowest-order outer solution*

Upon the substitution of (45) into (37) and equating terms of lowest order in ϵ, we obtain

$$\nabla_\rho^2 \hat{t}_0(\rho,\bar{\mu}) = Pr\left[\bar{\mu}\frac{\partial \hat{t}_0}{\partial \rho} + (1-\bar{\mu}^2)\frac{1}{\rho}\frac{\partial \hat{t}_0}{\partial \bar{\mu}}\right], \tag{47}$$

where
$$\nabla_\rho^2 = \frac{1}{\rho^2}\frac{\partial}{\partial \rho}\left(\rho^2\frac{\partial}{\partial \rho}\right) + \frac{1}{\rho^2}\frac{\partial}{\partial \bar{\mu}}(1-\bar{\mu}^2)\frac{\partial}{\partial \bar{\mu}}. \tag{48}$$

In (47) the convective term results from the freestream, which is the dominant velocity field as $r \to \infty$. The boundary condition as $r \to \infty$ is

$$\hat{t}_0(r\epsilon,\bar{\mu})|_{r\to\infty} = 0. \tag{49}$$

The solution for this set is given by Acrivos & Taylor (1962) and Fendell, Sprankle & Dodson (1966) as

$$\hat{t}_0(\rho,\bar{\mu}) = e^{\frac{1}{2}\rho Pr\bar{\mu}}\left(\frac{\pi}{\rho\, Pr}\right)^{\frac{1}{2}} \sum_{k=0}^{\infty} C_k\, K_{k+\frac{1}{2}}(\tfrac{1}{2}Pr\,\rho)\, P_k(\bar{\mu}), \tag{50}$$

where the spherical Bessel function may be written as

$$K_{k+\frac{1}{2}}(\tfrac{1}{2}Pr\rho) = \left(\frac{\pi}{\rho\,Pr}\right)^{\frac{1}{2}} e^{-\frac{1}{2}\rho Pr} \sum_{m=0}^{k} \frac{(k+m)!}{(k-m)!\,m!\,(\rho\,Pr)^m}. \tag{51}$$

For $\rho \to 0$ we have

$$K_{k+\frac{1}{2}}(\tfrac{1}{2}Pr\rho) \sim \left(\frac{\pi}{\rho\,Pr}\right)^{\frac{1}{2}} e^{-\frac{1}{2}\rho Pr} \frac{(2k)!}{k!\,(\rho\,Pr)^k}, \tag{52}$$

and hence

$$\hat{t}_0(\rho,\bar{\mu}) \sim e^{-\frac{1}{2}\rho Pr(1-\bar{\mu})} \left(\frac{\pi}{\rho\,Pr}\right) \sum_{k=0}^{\infty} C_k \frac{(2k)!}{k!\,(\rho\,Pr)^k} P_k(\bar{\mu}), \tag{53}$$

where the set of constants C_k is to be determined by matching with the inner solution.

3.3. *Lowest-order inner solution*

By substituting the expansion (39) into the governing equation (37) and equating terms to the leading order in ϵ, we obtain (Fendell *et al.* 1966)

$$\left(\nabla_r^2 - \frac{\tilde{A}_{00}}{r^2}\frac{\partial}{\partial r}\right) t_0(r,\bar{\mu}) = 0, \tag{54}$$

where

$$\nabla_r^2 = \frac{1}{r^2}\frac{\partial}{\partial r}\left(r^2\frac{\partial}{\partial r}\right) + \frac{1}{r^2}\frac{\partial}{\partial\bar{\mu}}(1-\bar{\mu}^2)\frac{\partial}{\partial\bar{\mu}},$$

$$\tilde{A}_{00} = Pr\,A_{00}.$$

By implementing

$$t_0(r,\bar{\mu}) = \sum_{m=0}^{\infty} l_{m0}(r)\,P_m(\bar{\mu}) \tag{55}$$

we obtain

$$r^2\frac{d^2 l_{m0}(r)}{dr^2} + (2r - \tilde{A}_{00})\frac{dl_{m0}(r)}{dr} - m(m+1)\,l_{m0}(r) = 0, \tag{56}$$

with boundary conditions

$$\left.\begin{array}{ll} l_{00}(1) = t_{i00}, & l_{m0}(1) = 0 \quad (m \geqslant 1), \\ \bar{l}_{00}(1) = w_{i00}, & l_{m0}(1) = 0 \quad (m \geqslant 1). \end{array}\right\} \tag{57}$$

The homogeneous boundary conditions for $m \geqslant 1$ relate to the fact that in the leading order ($\epsilon = 0$) we have no translation. Therefore complete spherical symmetry must exist at that order. A formal demonstration of this is possible through the matching with the dispersed phase for $\epsilon = 0$. The solution to (56) for $m = 0$ is

$$l_{00}(r) = Y_0 + (t_{i00} - Y_0)\frac{e^{-\tilde{A}_{00}/r} - 1}{e^{-\tilde{A}_{00}} - 1}, \tag{58}$$

and for $m \geqslant 1$ we have

$$l_{m0}(r) = Y_m\,[l_{m0}^{(1)}(r)\,l_{m0}^{(2)}(1) - l_{m0}^{(1)}(1)\,l_{m0}^{(2)}(r)]. \tag{59}$$

In (59) $l_{m0}^{(1)}(r)$ and $l_{m0}^{(2)}(r)$ are two linearly independent solutions given by

$$l_{m0}^{(1)} = \left(\sum_{k=0}^{m} a_{km}^{(1)}\,r^k\right), \tag{60}$$

$$l_{m0}^{(2)} = \left(\sum_{k=0}^{m} a_{km}^{(2)}\,r^k\right) e^{-\tilde{A}_{00}/r}. \tag{61}$$

The complete inner solution to the leading order is therefore given by

$$t_0(r,\bar{\mu}) = Y_0 + (t_{i00} - Y_0)\frac{e^{-\tilde{A}_{00}/r}-1}{e^{-\tilde{A}_{00}}-1} + \sum_{m=1}^{\infty} Y_m[l_{m0}^{(1)}(r)\,l_{m0}^{(2)}(1) - l_{m0}^{(1)}(1)\,l_{m0}^{(2)}(r)]\,P_m(\bar{\mu}). \quad (62)$$

The matching of the lowest-order inner and outer solution requires that

$$T(r\to\infty,\bar{\mu};\epsilon) = \hat{T}(\rho\to 0,\bar{\mu};\epsilon). \quad (63)$$

Thus we have

$$f_0(\epsilon)\,t_0(r\to\infty,\bar{\mu}) + O(f_1(\epsilon)) = F_0(\epsilon)\,\hat{t}_0(\rho\to 0,\bar{\mu}) + O(F_1(\epsilon)), \quad (64)$$

which may be written as

$$f_0(\epsilon)\left\{ Y_0 + \frac{t_{i00}-Y_0}{e^{-\tilde{A}_{00}}-1}\left(-\frac{\tilde{A}_{00}\,\epsilon}{\rho}+\dots\right) \right.$$

$$\left. + \sum_{m=1}^{\infty} Y_m\left[a_{0m}^{(1)}\frac{\rho^m}{\epsilon^m}l_{m0}^{(2)}(1) + O\left(\frac{1}{\epsilon^{m-1}}\right) \right]P_m(\bar{\mu}) \right\} + O(f_1(\epsilon))$$

$$= F_0(\epsilon)\left[(1-\tfrac{1}{2}Pr\rho(1-\bar{\mu})+\dots)\frac{\pi}{\rho\,Pr}\sum_{k=0}^{\infty} C_k\frac{(2k)!}{k!\,(\rho\,Pr)^k}P_k(\bar{\mu}) \right] + O(F_1(\epsilon)). \quad (65)$$

With $f_0(\epsilon) = 1$, the matching is accomplished up to order ϵ if

$$Y_0 = 0, \quad Y_m = 0 \quad (m \geqslant 1), \quad F_0(\epsilon) = \epsilon, \quad C_0 = \frac{-t_{i00}\,Pr\,\tilde{A}_{00}}{(e^{-\tilde{A}_{00}}-1)\,\pi}, \quad C_k = 0 \quad (k \geqslant 1). \quad (66)$$

The complete zeroth-order solutions are

$$f_0(\epsilon)\,t_0(r,\bar{\mu}) = t_{i00}\frac{e^{-\tilde{A}_{00}/r}-1}{e^{-\tilde{A}_{00}}-1}, \quad (67)$$

$$F_0(\epsilon)\,\hat{t}_0(\rho,\bar{\mu}) = -\frac{\epsilon t_{i00}\,\tilde{A}_{00}\,e^{-\frac{1}{2}Pr\rho(1-\bar{\mu})}}{\rho(e^{-\tilde{A}_{00}}-1)}, \quad (68)$$

$$\bar{f}_0(\epsilon)\,w_0(r,\bar{\mu}) = w_{i00}\frac{e^{-\tilde{A}'_{00}/r}-1}{e^{-\tilde{A}'_{00}}-1}, \quad (69)$$

$$\bar{F}_0(\epsilon)\,\hat{w}_0(\rho,\bar{\mu}) = -w_{i00}\frac{\epsilon\tilde{A}'_{00}\,e^{-\frac{1}{2}Sc\rho(1-\bar{\mu})}}{\rho(e^{-\tilde{A}'_{00}}-1)}, \quad (70)$$

where $\tilde{A}'_{00} = A_{00}\,Sc$.

3.4. *The next-order inner solution*

The governing equation given below is obtained by using the zeroth-order solution for the convective term in (37). We assume $f_1(\epsilon) = \epsilon$ and equate powers in ϵ^1. As a result we obtain

$$\frac{d^2 l_{m1}(r)}{dr^2} + \left(\frac{2}{r}-\frac{\tilde{A}_{00}}{r^2}\right)\frac{dl_{m1}(r)}{dr} - \frac{m(m+1)}{r^2}l_{m1}(r)$$

$$= \begin{cases} \dfrac{\tilde{A}_{01}}{r^2}\left[\dfrac{t_{i00}}{r^2}\tilde{A}_{00}\left(\dfrac{e^{-\tilde{A}_{00}/r}}{e^{-\tilde{A}_{00}}-1}\right)\right] \quad (m=0), & (71a) \\[4mm] Pr\left\{1+\dfrac{B}{r^3}+\dfrac{C}{r^2}\left[\dfrac{A_{00}}{r}\displaystyle\int_{1/A_{00}}^{r/A_{00}}(\xi^4+\xi^3)\,e^{-1/\xi}\,d\xi - \dfrac{1}{5}\left(\dfrac{r}{A_{00}}\right)^4 \right.\right. \\[3mm] \qquad\qquad\qquad \left.\left. +\dfrac{1}{6}\left(\dfrac{r}{A_{00}}\right)^2\right]\right\}\dfrac{t_{i00}\,\tilde{A}_{00}\,e^{-\tilde{A}_{00}/r}}{r^2(e^{-\tilde{A}_{00}}-1)} \quad (m=1), & (71b) \\[4mm] 0 \quad (m>1), & (71c) \end{cases}$$

where $\tilde{A}_{01} = A_{01} Pr$ and A_{01} is given by (20). The non-homogeneous terms for $m > 1$ do not show up, because the velocity field is calculated only up to $m = 1$. However, as discussed earlier, this formulation is completely valid up to order ϵ.

Case $m = 0$. The boundary conditions are

$$l_{01}(1) = t_{i01}, \quad \bar{l}_{01}(1) = w_{i01}. \tag{72}$$

By the variation-of-parameters technique we obtain

$$l_{01}(r) = -\frac{\tilde{C}}{\tilde{A}_{00}^2}\left[e^{-\tilde{A}_{00}/r}\left(1 + \frac{\tilde{A}_{00}}{r}\right)\right] + C_{11}\,e^{-\tilde{A}_{00}/r} + C_{12}, \tag{73}$$

where C_{11} and C_{12} are related by the boundary condition (72). Thus

$$t_{i01} = -\frac{\tilde{C}}{\tilde{A}_{00}^2}[e^{-\tilde{A}_{00}}(1 + \tilde{A}_{00})] + C_{11}\,e^{-\tilde{A}_{00}} + C_{12}, \tag{74}$$

with $$\tilde{C} = \frac{\tilde{A}_{01}\,\tilde{A}_{00}\,t_{i00}}{e^{-\tilde{A}_{00}} - 1}.$$

The integration constants C_{11} and C_{12} would be completely determined by the asymptotic matching, taken together with the relationship (74).

Case $m = 1$. The boundary conditions are

$$l_{11}(1) = t_{i11}, \quad \bar{l}_{11}(1) = w_{i11}. \tag{75}$$

Again by the method of variation of parameters we obtain

$$l_{11}(r) = [C_{21} + \overline{V}(r)]\,e^{-\tilde{A}_{00}/r}(r + \tfrac{1}{2}\tilde{A}_{00}) + [C_{22} + \overline{U}(r)]\,(r - \tfrac{1}{2}\tilde{A}_{00}), \tag{76}$$

where

$$\overline{U}(r) = \frac{4\hat{\alpha}}{\tilde{A}_{00}^3}\int_1^r (r' + \tfrac{1}{2}\tilde{A}_{00})\left\{1 + \frac{B}{r'^3} + \frac{C}{r'^2}\left[\frac{A_{00}}{r'}\int_{1/A_{00}}^{r'/A_{00}} (\xi^4 + \xi^3)\,e^{-1/\xi}\,\mathrm{d}\xi\right.\right.$$

$$\left.\left. -\frac{1}{5}\left(\frac{r'}{A_{00}}\right)^4 + \frac{1}{6}\left(\frac{r'}{A_{00}}\right)^2\right]\right\}e^{-\tilde{A}_{00}/r'}\,\mathrm{d}r', \tag{77}$$

$$\overline{V}(r) = -\frac{4\hat{\alpha}}{\tilde{A}_{00}^3}\int_1^r (r' - \tfrac{1}{2}\tilde{A}_{00})\left\{1 + \frac{B}{r'^3} + \frac{C}{r'^2}\left[\frac{A_{00}}{r'}\int_{1/A_{00}}^{r'/A_{00}} (\xi^4 + \xi^3)\,e^{-1/\xi}\,\mathrm{d}\xi\right.\right.$$

$$\left.\left. -\frac{1}{5}\left(\frac{r'}{A_{00}}\right)^4 + \frac{1}{6}\left(\frac{r'}{A_{00}}\right)^2\right]\right\}\mathrm{d}r', \tag{78}$$

where $\hat{\alpha}$ is defined as

$$\hat{\alpha} = \frac{Pr\,t_{i00}\,\tilde{A}_{00}}{e^{-\tilde{A}_{00}} - 1}.$$

The integration constants C_{21} and C_{22} are related through the boundary condition (75). The relationship is

$$t_{i11} = C_{21}\,e^{-\tilde{A}_{00}}(1 + \tfrac{1}{2}\tilde{A}_{00}) + C_{22}(1 - \tfrac{1}{2}\tilde{A}_{00}). \tag{79}$$

An additional relationship is obtained through matching the inner solution with the outer solution. The matching principle consists of the requirement that

$$t_0(r \to \infty, \bar{\mu}) + \epsilon t_1(r \to \infty, \bar{\mu}) = \epsilon \hat{t}_0(\rho \to 0, \bar{\mu}). \tag{80}$$

Such a procedure calls for the asymptotic expansions of $l_{01}(r)$ and $l_{11}(r)$. The expansion for $l_{01}(r)$ is obtained in a quite-straightforward manner as

$$l_{01}\left(\frac{\rho}{\epsilon}\right) \sim \left(C_{11}+C_{12}-\frac{\tilde{C}}{\tilde{A}_{00}^2}\right)-\epsilon C_{11}\frac{\tilde{A}_{00}}{\rho}+O\left(\frac{\epsilon^2}{\rho^2}\right). \tag{81}$$

A great deal of algebra gives the expansion for $l_{11}(\rho/\epsilon)$ as

$$l_{11}\left(\frac{\rho}{\epsilon}\right) \sim \frac{\hat{\alpha}}{\tilde{A}_{00}}\left[1+\Omega+\frac{\tilde{A}_{00}}{\hat{\alpha}}(C_{21}+C_{22})\right]\frac{\rho}{\epsilon}-\hat{\alpha}\left[1+\tfrac{1}{2}\Omega+\frac{\tilde{A}_{00}}{2\hat{\alpha}}(C_{21}+C_{22})\right]+O\left(\frac{\epsilon}{\rho}\right), \tag{82}$$

where Ω is a constant given by

$$\Omega = \frac{2B}{A_{00}^2 Pr^2}\left[\frac{3}{A_{00} Pr}-2(1-\tfrac{1}{4}A_{00} Pr)-\left(1+\frac{3}{A_{00} Pr}\right)e^{-A_{00} Pr}\right]$$

$$-\frac{2C}{A_{00}^2 Pr^2}\left\{2\left[\tfrac{1}{120}Pr^3-\tfrac{1}{240}Pr^2+\tfrac{11}{120}Pr+\frac{Pr}{60(1+Pr)}+\frac{1}{60Pr}\right.\right.$$

$$-\frac{1}{20Pr}(Ei(-A_{00})-\gamma-\ln(-A_{00}))+\frac{3e^{-A_{00}}}{10Pr A_{00}^5}(1+A_{00}-\tfrac{1}{3}A_{00}^2+\tfrac{1}{6}A_{00}^3-\tfrac{1}{6}A_{00}^4)\Big]$$

$$-\left[\left(\left(\frac{3}{5A_{00}^5 Pr}+\frac{1}{4A_{00}^4}+\frac{3}{4A_{00}^4 Pr}+\frac{1}{3A_{00}^3}\right)\right.\right.$$

$$-\left(\frac{3}{20A_{00}^4 Pr}+\frac{1}{12A_{00}^3}+\frac{1}{4A_{00}^3 Pr}+\frac{1}{6A_{00}^2}\right)(1+Pr)$$

$$+\left(\frac{1}{20A_{00}^3 Pr}+\frac{1}{24A_{00}^2}+\frac{1}{8A_{00}^2 Pr}+\frac{1}{6A_{00}}\right)(1+Pr)^2$$

$$-\left(\frac{1}{40A_{00}^2 Pr}+\frac{1}{24A_{00}}+\frac{1}{8A_{00} Pr}\right)(1+Pr)^3+\frac{(1+Pr)^4}{40A_{00} Pr}\right)e^{-A_{00}(1+Pr)}$$

$$+\left(\frac{(1+Pr)^5}{40Pr}-\tfrac{1}{24}(1+Pr)^4-\frac{(1+Pr)^4}{8Pr}+\tfrac{1}{6}(1+Pr)^3\right)(Ei(-A_{00}(1+Pr))$$

$$-\gamma-\ln(-A_{00}(1+Pr))\Big]-\left[\left(\frac{1}{10A_{00}^4}+\frac{Pr}{30A_{00}^3}-\frac{Pr^2}{60A_{00}^2}\right.\right.$$

$$-\frac{1}{6A_{00}^2}+\frac{Pr^3}{60A_{00}}\right)e^{-A_{00} Pr}+\tfrac{1}{60}Pr^4(Ei(-A_{00} Pr)-\gamma-\ln(-A_{00} Pr))\Big]$$

$$+\left[\left((-\tfrac{1}{2}+\tfrac{1}{6}A_{00} Pr)\frac{1}{A_{00}^4}-(\tfrac{1}{2}-\tfrac{1}{6}A_{00} Pr)\frac{1}{A_{00}^3}+(\tfrac{1}{4}-\tfrac{1}{6}A_{00} Pr)\frac{1}{A_{00}^2}-\frac{1}{4A_{00}}\right)e^{-A_{00}}\right.$$

$$-(\tfrac{1}{4}+\tfrac{1}{6}Pr)(Ei(-A_{00})-\gamma-\ln(-A_{00}))\Big]-\frac{1}{15}\sum_{n=1}^{\infty}\left(\frac{n+3}{2n}\right)\left(-\frac{1}{Pr}\right)^{n+1}$$

$$+\left(\frac{1}{10A_{00}^4}-\frac{Pr}{15A_{00}^3}-\frac{1}{6A_{00}^2}+\frac{Pr}{6A_{00}}\right)\right\}+\frac{2}{A_{00}^2 Pr^2}(1-e^{-A_\infty Pr}-A_{00} Pr). \tag{83}$$

Here

$$Ei(-x) = -\int_x^\infty \frac{e^{-x_1}}{x_1}dx_1$$

is the exponential integral and $\gamma = 0.57721\ldots$ is the Euler–Mascheroni constant.

After carefully applying the matching condition (80) up to and including $O(\epsilon)$ terms, we obtain the following relationships:

$$-\frac{\tilde{C}}{\tilde{A}_{00}^2} + C_{11} + C_{12} = \frac{\tilde{A}_{00}\, t_{i00}\, Pr}{2(e^{-\tilde{A}_{00}} - 1)}, \tag{84}$$

$$1 + \Omega + \frac{\tilde{A}_{00}}{\hat{\alpha}}(C_{21} + C_{22}) = 0. \tag{85}$$

The use of these relationships, along with (74) and (79), yields

$$C_{11} = \frac{t_{i01}}{e^{-\tilde{A}_{00}} - 1} - \frac{\tilde{A}_{00}\, t_{i00}}{(e^{-\tilde{A}_{00}} - 1)^2}\left\{\tfrac{1}{2}Pr + \frac{\tilde{A}_{01}}{\tilde{A}_{00}^2}[1 - e^{-\tilde{A}_{00}}(1 + \tilde{A}_{00})]\right\}, \tag{86a}$$

$$C_{12} = \frac{e^{-\tilde{A}_{00}}\, \tilde{A}_{00}\, t_{i00}}{(e^{-\tilde{A}_{00}} - 1)^2}\left[\tfrac{1}{2}Pr - \frac{\tilde{A}_{01}}{\tilde{A}_{00}} - \frac{t_{i01}}{e^{-\tilde{A}_{00}} - 1}\right], \tag{86b}$$

$$C_{21} = -\frac{\dfrac{\hat{\alpha}}{\tilde{A}_{00}}(1 + \Omega)(1 - \tfrac{1}{2}\tilde{A}_{00}) + t_{i11}}{1 - \tfrac{1}{2}\tilde{A}_{00} - e^{-\tilde{A}_{00}}(1 + \tfrac{1}{2}\tilde{A}_{00})}, \tag{86c}$$

$$C_{22} = \frac{\dfrac{\hat{\alpha}}{\tilde{A}_{00}}(1 + \Omega)(1 + \tfrac{1}{2}\tilde{A}_{00})\, e^{-\tilde{A}_{00}} + t_{i11}}{1 - \tfrac{1}{2}\tilde{A}_{00} - e^{-\tilde{A}_{00}}(1 + \tfrac{1}{2}\tilde{A}_{00})} \tag{86d}$$

For the species equations, the solutions are identical with the above temperature solutions except that t_{i00}, t_{i11} should be replaced by w_{i00}, w_{i01} and w_{i11}, respectively. The quantities $\tilde{A}_{00}$ and $\tilde{A}_{01}$ should be replaced by $\tilde{A}_{00}' = \tilde{A}_{00}\,Sc$ and $\tilde{A}_{01}' = \tilde{A}_{01}\,Sc$ respectively. In the expression for Ω we replace Pr by Sc.

Next the compatibility equations (31c) and (35c) are used to obtain relationships between the interfacial mass fractions and the normal velocities. We note here that the relationships between m_i and $w(1, \bar{\mu}; \epsilon)$ are

$$m_{i0} = w_{i00} + m_{\infty}, \quad m_{i1} = w_{i01} + \bar{\mu}w_{i11}. \tag{87}$$

The use of (31c) leads to

$$\tilde{A}_{00}'(w_{i00} + m_{\infty}) = \left.\frac{\mathrm{d}\bar{l}_{00}(r)}{\mathrm{d}r}\right|_{r-1}, \tag{88}$$

and (35c) gives

$$\tilde{A}_{00}'(w_{i01} + \bar{\mu}w_{i11}) + (\tilde{A}_{01}' + \tilde{A}_{11}'\bar{\mu})(w_{i00} + m_{\infty}) = \left\{\frac{\mathrm{d}}{\mathrm{d}r}[\bar{l}_{01}(r) + \bar{\mu}\bar{l}_{11}(r)]\right\}_{r-1}. \tag{89}$$

Upon equating powers in $\bar{\mu}$, we may write (89) as

$$\tilde{A}_{00}'\, w_{i01} + \tilde{A}_{01}'(w_{i00} + m_{\infty}) = \left.\frac{\mathrm{d}\bar{l}_{01}(r)}{\mathrm{d}r}\right|_{r-1}, \tag{90}$$

$$\tilde{A}_{00}'\, w_{i11} + \tilde{A}_{11}'(w_{i00} + m_{\infty}) = \left.\frac{\mathrm{d}\bar{l}_{11}(r)}{\mathrm{d}r}\right|_{r-1}. \tag{91}$$

The substitution of $\bar{l}_{00}(r)$, $\bar{l}_{01}(r)$ and $\bar{l}_{11}(r)$ into the above equations yields

$$A_{00} = -\frac{1}{Sc}\ln\left(1 + \frac{w_{i00}}{m_{\infty}}\right), \tag{92}$$

$$A_{01} = \frac{e^{-\tilde{A}_{00}'}}{Sc(w_{i00} + m_{\infty})}\{-w_{i01}\tilde{A}_{00}'\, e^{\tilde{A}_{00}'} + [-\tilde{C}^* + C_{11}^*\tilde{A}_{00}']\}, \tag{93}$$

$$A_{11} = \frac{1}{Sc} \frac{C_{21}^*\{1 + (1 + \frac{1}{2}\tilde{A}_{00}') \tilde{A}_{00}'\} e^{-\tilde{A}_{00}'} + C_{22}^* - \tilde{A}_{00}' w_{i11}}{w_{i00} + m_\infty}, \tag{94}$$

where $\tilde{C}^*$, C_{21}^* and C_{22}^* represent the constants similar to $\tilde{C}$, C_{21} and C_{22} respectively, with Pr changed to Sc and t_{imn} changed to w_{imn}.

This concludes the singular perturbation solution for the continuous phase when Re_c is as much as $O(1)$.

In §4 we shall examine the special limit where the normal velocity becomes small enough so that the entire flow field is in the Stokes regime. Such a situation would arise when the mass fraction of the non-condensable component in the bulk is rather large and the condensation rate is low.

4. The limit of low condensation rates

In the limit of A_{00} becoming small it can be shown that the flow field collapses to Stokes flow (Sadhal & Ayyaswamy 1983). As a result considerable simplicity in the mathematical structure of the problem is realized. Since such a situation is of practical interest (presence of a large amount of the non-condensable component in a condensing situation) we choose to provide results appropriate to that limit. This limiting solution may be obtained either by letting A_{00} become vanishingly small in the previous development, or by formally carrying out the singular perturbation procedure using A_{00} as a second small parameter along with ϵ. It turns out that the latter procedure is considerably simpler than the former. The results are as follows.

Lowest-order solutions

The complete zeroth-order solutions corresponding to (67)–(70) are

inner

$$f_0(\epsilon) t_0(r, \bar{\mu}) = \frac{t_{i00}}{r}; \tag{95}$$

outer

$$F_0(\epsilon) \hat{t}_0(r, \bar{\mu}) = \frac{\epsilon t_{i00} e^{-\frac{1}{2}\rho Pr(1 - \bar{\mu})}}{\rho}. \tag{96}$$

The next-order inner solutions

The solutions corresponding to (73) and (76) are

$$l_{01}(r) = -\frac{1}{2} t_{i00} Pr + (t_{i01} + \frac{1}{2}\tilde{A}_{00} t_{i00} + \frac{1}{2} t_{i00} Pr) \frac{1}{r} - \frac{\tilde{A}_{00} t_{i00}}{2r^2}, \tag{97}$$

$$l_{11}(r) = t_{i11} + \frac{3}{8} \frac{Pr\, t_{i00}}{(1 + \phi_\mu)} \frac{1}{r^2} + Pr\, t_{i00} \left(\frac{1}{2} - \frac{1}{8r^3(1 + \phi_\mu)} - \frac{3 + 2\phi_\mu}{4r(1 + \phi_\mu)}\right). \tag{98}$$

The solutions for the species equations are identical with (95)–(98) except that we replace Pr by Sc, t_{imn} by w_{imn} and $\tilde{A}_{mn}$ by $\tilde{A}_{mn}'$.

We now use the compatibility condition (13d) to obtain relationships between the interfacial mass fractions and the normal velocities. We treat both A_{00} and ϵ as small, but distinctly independent, parameters. Consequently we obtain

$$A_{00} = \frac{-w_{i00}}{Sc(w_{i00} + m_\infty)}, \tag{99}$$

$$A_{01} = -\frac{(1 + \tilde{A}_{00}') w_{i01} - \frac{1}{2}\tilde{A}_{00}' w_{i00} + \frac{1}{2} w_{i00} Sc}{Sc(w_{i00} + m_\infty)}, \tag{100}$$

$$A_{11} = \frac{Sc\, w_{i00}\dfrac{3+4\phi_\mu}{8(1+\phi_\mu)} - \tilde{A}'_{00}\, w_{i11}}{Sc(w_{i00}+m_\infty)}. \tag{101}$$

The examination of (92)–(94) and (99)–(101) shows that the interfacial velocities are functions of the mass fractions at that location. These are strongly related to the temperature and the composition. Therefore a transient solution of the condensed liquid phase is necessary to provide the surface temperature, and the continuous phase and condensed phase are connected through the energy-flux continuity equation (13*e*). The details of numerical matching of this energy flux are presented in §5.

5. Transient heat-up of the drop interior

The flow field for the droplet inside is given by (23) and (24). With this, the dimensionless energy equation given by (10*c*) may be written as

$$\frac{\partial T_\ell}{\partial t} + \hat{B}\, Re_\ell\, Pr_\ell \left[(r^2-1)\,\bar{\mu}\,\frac{\partial T_\ell}{\partial r} + \frac{1}{r}(2r^2-1)\,(1-\bar{\mu}^2)\,\frac{\partial T_\ell}{\partial\bar{\mu}} \right] = \nabla_r^2\, T_\ell, \tag{102}$$

where $\hat{B}$ is given by (27). The initial and boundary conditions are

$$T_\ell = 1 \quad (t=0;\ \text{all}\ r,\theta), \tag{103}$$

$$\left.\begin{aligned}
& T_\ell < \infty \quad (r\to 0;\ \text{all}\ \theta, t>0), \\[2mm]
& \frac{\partial T_\ell}{\partial\theta} = 0 \quad (\theta=0,\pi;\ \text{all}\ r, t>0), \\[2mm]
& \frac{\partial T_\ell}{\partial r} = \phi_k\left(-\frac{Pr}{Ja}\boldsymbol{u}\cdot\boldsymbol{n} + \frac{\partial T}{\partial r} \right) \quad (r=1;\ t>0).
\end{aligned}\right\} \tag{104}$$

We adopt the semi-analytical method of series truncation for the solution of this equation. The fluid temperature is expressed as an expansion series in Reynolds number and Legendre polynomials. As demonstrated by Dennis, Walker & Hudson (1973), the number of terms to be used is associated with the expansion parameter. Since the Péclet number is small only a few terms are required. We shall develop a three-term expansion series, viz

$$T_\ell = T_{\ell 00} + \epsilon(T_{\ell 01} + \bar{\mu}T_{\ell 11}). \tag{105}$$

Substituting (105) into (102) and equating terms of the same order, we obtain

$$\left.\begin{aligned}
& \frac{\partial T_{\ell 00}}{\partial t} = \frac{\partial^2 T_{\ell 00}}{\partial r^2} + \frac{2}{r}\frac{\partial T_{\ell 00}}{\partial r}, \\[2mm]
& \frac{\partial T_{\ell 01}}{\partial t} = \frac{\partial^2 T_{\ell 01}}{\partial r^2} + \frac{2}{r}\frac{\partial T_{\ell 01}}{\partial r}, \\[2mm]
& \frac{\partial T_{\ell 01}}{\partial t} = -\hat{B}\phi_\nu\, Pr_\ell(r^2-1)\frac{\partial T_{\ell 00}}{\partial r} + \frac{\partial^2 T_{\ell 11}}{\partial r^2} + \frac{2}{r^2}\frac{\partial T_{\ell 11}}{\partial r} - \frac{2T_{\ell 11}}{r^2}.
\end{aligned}\right\} \tag{106}$$

These are subject to

$$T_{\ell 00} = 1, \quad T_{\ell 01} = T_{\ell 11} = 0 \quad (t=0;\ \text{all}\ r,\theta), \tag{107}$$

$$\frac{\partial T_{\ell 00}}{\partial r} = \frac{\partial T_{\ell 01}}{\partial r} = T_{\ell 11} = 0 \quad (r = 0; \text{ all } \theta, t > 0). \tag{108}$$

The appropriate compatibility equations at the interface are

$$\left.\begin{array}{l} \dfrac{\partial T_{\ell 00}}{\partial r} = -\dfrac{\phi_k Pr}{Ja} A_{00} + \phi_k \dfrac{\partial T_{00}}{\partial r}, \\[3mm] \dfrac{\partial T_{\ell 01}}{\partial r} = \phi_k\left(-\dfrac{Pr}{Ja} A_{01} + \dfrac{\partial T_{01}}{\partial r}\right), \\[3mm] \dfrac{\partial T_{\ell 11}}{\partial r} = \phi_k\left(-\dfrac{Pr}{Ja} A_{11} + \dfrac{\partial T_{11}}{\partial r}\right). \end{array}\right\} \tag{109}$$

Equations (106), with corresponding initial and boundary conditions, have been solved numerically through an efficient finite-difference method. We employ central-difference expressions for the spatial derivatives and backward-difference expressions for the temporal derivatives. This ensures a second-order accuracy in space and obtains unconditionally stable solutions. The finite-difference equations for (106) are written as

$$T_i^{n+1} = a_{1i} T_{i+1}^{n+1} + a_{2i} T_{i-1}^{n+1} + a_{3i} \quad (i = 1, 2, \ldots, L-1), \tag{110}$$

where T represents $T_{\ell 00}$, $T_{\ell 01}$ or $T_{\ell 11}$. The subscript i is the node-point designation. The drop interior is divided into $L-1$ equal spacings, with $i = 1$ corresponding to the centre of the drop and $i = L$ corresponding to the drop surface. The superscript represents the time-step number. The finite-difference equation for the surface node is formulated on the basis of the set of equations (109) together with an energy balance over a one-half-size element adjacent to the surface. This becomes

$$T_L^{n+1} = \frac{2(\sigma_1 + \sigma_2)}{\sigma} T_{L-1}^{n+1} + \frac{2(\sigma_1 + \sigma_2)}{\sigma} \Delta r \frac{\partial T_L^n}{\partial r} + \frac{T_L^n}{\sigma}, \tag{111}$$

where T stands for $T_{\ell 00}$, $T_{\ell 01}$ and $T_{\ell 11}$; $\sigma_1 = \Delta t/\Delta r^2$, $\sigma_2 = \Delta t/\Delta r$, and $\sigma = 1 + 2\sigma_1$ for $T = T_{\ell 00}$ or $T_{\ell 01}$, $\sigma = 1 + 2\sigma_1 + 2\Delta t$ for $T = T_{\ell 11}$. The time-step size and the space-step size are Δt and Δr respectively. In (111) the term $\partial T_L^n/\partial r$ is evaluated from the set of equations (109). With the right-hand sides of (109) known from the continuous-phase analysis, (110) and (111) can be solved by a tridiagonal matrix algorithm. The solution will provide an updated temperature profile for both the drop surface and its interior. With this new drop-surface-temperature solution, the continuous-phase calculation for the new time step may be effected.

6. Heat transfer

The local heat flux at the interface is given by

$$\dot{q} = \dot{m}\lambda - k\frac{\partial T}{\partial r}\bigg|_i = \rho \boldsymbol{u} \cdot \boldsymbol{n}\lambda - k\frac{\partial T}{\partial r} = \rho U_\infty \boldsymbol{u}^* \cdot \boldsymbol{n}\lambda - k\frac{\Delta T}{R}\frac{\partial T^*}{\partial r^*}. \tag{112}$$

The total heat-transfer rate is given by

$$\dot{Q} = \int_0^\pi \dot{q}\, 2\pi R^2 \sin\theta\, d\theta. \tag{113}$$

We can define an average based on the surface area of the drop as

$$\bar{q} = \dot{Q}/4\pi R^2. \tag{114}$$

For high condensation rates ($Re_c = O(1)$) this average is

$$\bar{q} = \rho U_\infty \left(\frac{A_{00}}{\epsilon} + A_{01} \right) \lambda - k \frac{\Delta T}{R} \left\{ \frac{-t_{i00} \tilde{A}_{00} e^{-\tilde{A}_{00}}}{e^{-\tilde{A}_{00}} - 1} + \epsilon[-\tilde{C} e^{-\tilde{A}_{00}} + C_{11} \tilde{A}_{00} e^{-\tilde{A}_{00}}] \right\}. \tag{115}$$

Here A_{00}, A_{01}, $\tilde{C}$ and C_{11} are given by (92), (93), (74b) and (86a) respectively. The leading-order interface temperature t_{i00} is obtained through matching at the interface. For low rates of condensation we can write a similar expression for the average heat transfer as

$$\bar{q} = \rho U_\infty (A_{00} + \epsilon A_{01}) \lambda - k \frac{\Delta T}{R} \{ -t_{i00} + \epsilon[-t_{i01} + \tfrac{1}{2}\tilde{A}_{00} t_{i00} - \tfrac{1}{2} t_{i00} Pr] \}. \tag{116}$$

In (116) A_{00} and A_{01} are given by (99) and (100) respectively. To exhibit the effects of the presence of the non-condensable gas and the forced flow explicitly, we shall present some of the heat-transfer results in terms of the variations of the dimensionless heat-flux ratio $\bar{q}/\bar{q}_{Nu}$. The heat flux $\bar{q}_{Nu}$ is the average heat flux corresponding to a 'Nusselt-type' condensation heat transfer to an isothermal solid sphere situated in an atmosphere of quiescent, pure, saturated steam. The temperature of the solid sphere is set equal to the initial temperature T_0 of the drop. An expression for $\bar{q}_{Nu}$ has been given by Yang (1973):

$$\bar{q}_{Nu} = 0.803 \left(\frac{g(\rho_\ell - \rho_\infty) \lambda k_\ell^3 (T_\infty - T_0)^3}{2R\nu_\ell} \right)^{\frac{1}{4}}. \tag{117}$$

To assess the effect of drop translation on heat transfer we will examine the ratio $\bar{q}/\bar{q}_{(\epsilon = 0)}$ as a function of time. Here $\bar{q}_{(\epsilon = 0)}$ is the average heat flux to a stationary drop situated in otherwise identical conditions experienced by the moving drop. It is easy to show that

$$\bar{q}_{(\epsilon = 0)} = \frac{\mu_\infty A_{00}}{R} \lambda - k \frac{\Delta T}{R} \left\{ \tilde{A}_{00} \frac{e^{-\tilde{A}_{00}}}{e^{-\tilde{A}_{00}} - 1} \right\}. \tag{118}$$

Additionally we define a dimensionless overall conductance $\mathcal{U}$, based on the difference between the far-stream temperature T_∞ and the instantaneous average temperature $T_{av}(t)$ of the drop. $T_{av}(t)$ could be regarded as the instantaneous mixing-cup temperature of the drop. Thus

$$\mathcal{U} = \frac{\bar{q} R}{k(T_\infty - T_{av}(t))}. \tag{119}$$

7. Results and discussion

Quasi-steady condensation heat/mass transfer in the continuous phase and transient heat-up of the drop interior have been examined for a small drop that is falling in a mixture of steam and air. In this study both the viscous and inertial effects have been included in the treatment of the problem. The present analysis therefore represents an advance on previous analyses of problems with analogous descriptions of the transport (e.g. Fendell et al. 1966).

First we establish the fall velocity of the drop. The fall velocity, at any instant, will depend on the strength of the interfacial radial velocity that is induced by condensation. We can estimate the instantaneous velocity of the drop in a quasi-steady
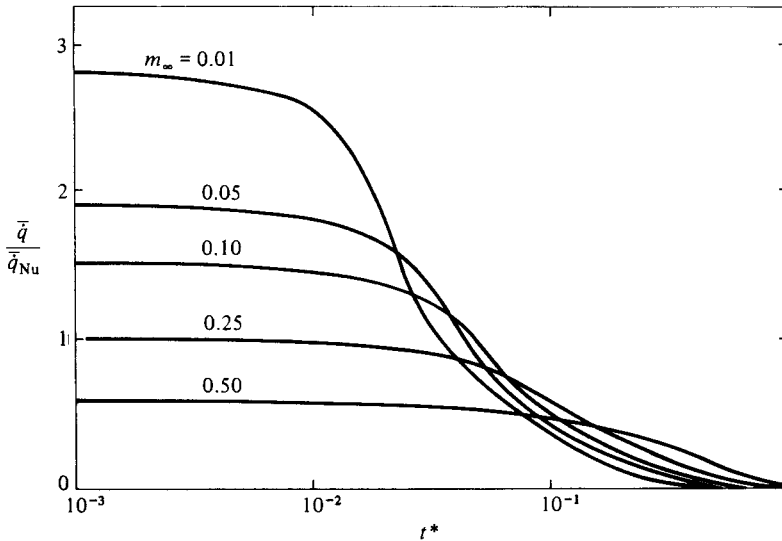
FIGURE 2. The effect of the non-condensable gas on dimensionless heat transfer;
$Re_{nc} = 0.5$, $T_0 = 30$ °C, $T_\infty = 100$ °C.

condensing situation through a balance between drag and gravity forces. Sadhal &
Ayyaswamy (1983) have calculated the drag experienced by a moving drop in a strong
radial flow field. Based on that development, the instantaneous fall velocity is

$$U_\infty(t) = \frac{(\rho_\ell - \rho_\infty)gR^2}{\left(3A_{00} + \dfrac{C}{2A_{00}}\right)\mu_\infty}.$$ (120)

For a non-condensing situation

$$U_{\infty 0} = \frac{2(\rho_\ell - \rho_\infty)}{3\mu_\infty}\frac{\mu_\ell + \mu_\infty}{2\mu_\infty + 3\mu_\ell}gR^2.$$ (121)

Equation (121) can be deduced either from (120) or from the Hadamard–Rybczynski
solution. In figures 2–9, we have presented results using (120) in evaluating the
various quantities. At several places we have indicated the value of a time-independent
Reynolds number Re_{nc}. This Re_{nc} is the Reynolds number based on the steady
terminal velocity $U_{\infty 0}$ given by (121) and characterizes the condition when the moving
drop has thermalized with its outside environment (no-condensation situation). We
choose to report our results in this manner because the instantaneous value of the
actual Reynolds number $Re_\infty(t)$ itself varies with the drop-translation history and
is therefore an unsuitable parameter for discussing the results. In figure 10 we have
plotted the variation of the instantaneous Reynolds number with time for the sake
of completeness. For illustration purposes, we take the droplet initial temperature
to be 30 °C. The drop environment consists of air saturated with steam, with the air
mass fraction ranging from 0.01 to 0.5. The ambient temperatures range between
100 °C and 150 °C and the Reynolds numbers Re_{nc} are in the range 0.05–0.5.

Figure 2 shows the effect of the presence of the non-condensable gas. The curves
give $\bar{q}/\bar{q}_{Nu}$ as a function of dimensionless time t^* for various m_∞. In the high-
condensation regime, at $t^* = 10^{-3}$, the dimensionless heat transfer drops from 2.8 to
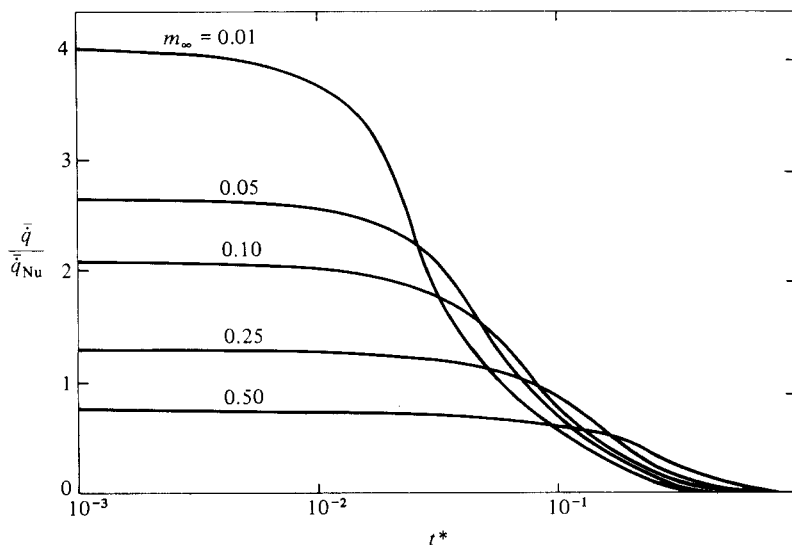almost half its value as the mass fraction of air increases from 0.01 to 0.1. In the

FIGURE 3. The effect of the non-condensable gas on dimensionless heat transfer;
$Re_{nc} = 0.1$, $T_0 = 30\ ^{\circ}\mathrm{C}$, $T_{\infty} = 100\ ^{\circ}\mathrm{C}$.

low-condensation regime $\bar{q}/\bar{q}_{\mathrm{Nu}}$ is a mere 0.6 for $m_{\infty} = 0.5$. For the parameters used here $\bar{q}_{\mathrm{Nu}} = 250\ \mathrm{W/cm^2}$. The reason for the reduction in heat transfer due to the presence of the non-condensable component is that a build-up of the non-condensable gas at the interface causes a reduction in the partial pressure of the vapour at the interface. In turn, this reduces the saturation temperature at which the condensation takes place. The net effect is to lower the effective thermal driving force $T_{\mathrm{i}} - T_0$, thereby reducing the heat transfer. It is also evident from figure 2 that the dimensionless heat-transfer rate is significantly influenced by the surface temperature of the drop. For example it is seen that, for $m_{\infty} = 0.01$ (low concentration of non-condensable component in the bulk), the rate of decrease of heat transfer with increasing time is actually higher than for, say, $m_{\infty} = 0.05$ or $m_{\infty} = 0.1$ situations, beyond a dimensionless time of about 10^{-2}. The liquid drop in a lower-m_{∞} environment initially experiences a relatively more vigorous heat transfer. This results in a rapid increase of the surface temperature and consequently the thermal driving force $T_{\infty} - T_{\mathrm{i}}$ decreases faster as a function of time. The heat-transfer rate decreases with a steeper slope. This suggests that, although the non-condensable gas mass fraction in the bulk may be higher, the time-dependent condensation rate may still be higher in certain stages of the transient process. Based merely on the extent of non-condensable component in the environment, no definitive conclusion can be drawn as to the rates of heat transfer for a drop experiencing condensation in a forced flow field. In figure 3 all the parameters are the same as in figure 2 except that the Reynolds number Re_{nc} is equal to 0.1. The rate of decrease of the dimensionless heat transfer is considerably higher and the droplet equilibrates with the environment in a relatively very short time. This is as would be expected, in view of the lower terminal velocity for the droplet motion. We shall discuss this feature later in reference to figure 7. The reduction of heat transfer due exclusively to the presence of the non-condensable gas can be discerned from an examination of the early-stage transport given in figure 4. At $t^* = 10^{-3}$ the bulk temperatures of the droplets for the various cases studied are almost the same and not very much different from the temperature at introduction
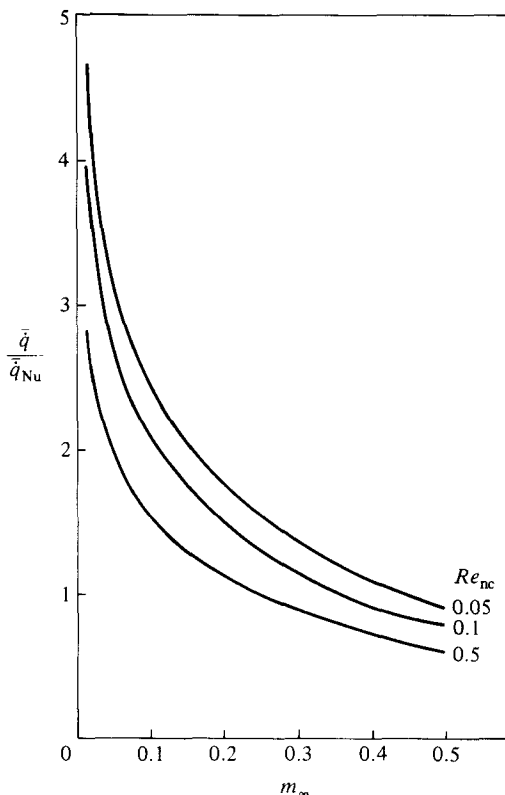
FIGURE 4. The reduction in dimensionless heat transfer as a function of non-condensable gas concentration; $T_0 = 30$ °C, $T_\infty = 100$ °C, $t^* = 10^{-3}$.

(about 30 °C). The presence of the non-condensable gas is seen to be the dominant factor for the reduction in heat transfer.

Forced flow enhances condensation heat transfer both by providing a mechanism for the removal of non-condensable from the drop surface, and by convective transport via internal circulation. The non-condensable gas forms a resistive layer which inhibits condensation. With higher non-condensable mass fraction in the bulk, the effect of drop translation becomes more significant. Also, for a moving drop, the condensation-induced velocity will decrease continuously with time. The drop gets progressively hotter and the corresponding thermal driving force becomes smaller, but the translational velocity of the drop will decrease continuously with time until thermal equilibrium with the outside environment is achieved (condensation ceases). Beyond thermal equilibrium, the drop would move at a constant speed. We should therefore expect a continuous increase in the translational effect on heat transfer until thermalization. From figure 5 we see that the $\dot{q}/\dot{q}_{(\epsilon\,=\,0)}$ characteristic has an increasing slope for, say, $10^{-3} < t^* < 2.5 \times 10^{-2}$, $m_\infty = 0.01$. Beyond about $t^* = 2.5 \times 10^{-2}$ a decrease in $\bar{q}/\bar{q}_{(\epsilon\,=\,0)}$ is observed. This may be explained when we note that, for a very small non-condensable mass fraction in the bulk (such as $m_\infty = 0.01$), a moving drop would experience vigorous heat transfer in the early stages of motion. It equilibrates sooner than an equivalent stationary drop. The net effect is a decrease in $\bar{q}/\bar{q}_{(\epsilon\,=\,0)}$ beyond $t^* = 2.5 \times 10^{-2}$. Similar features may also hold for higher values of m_∞, and
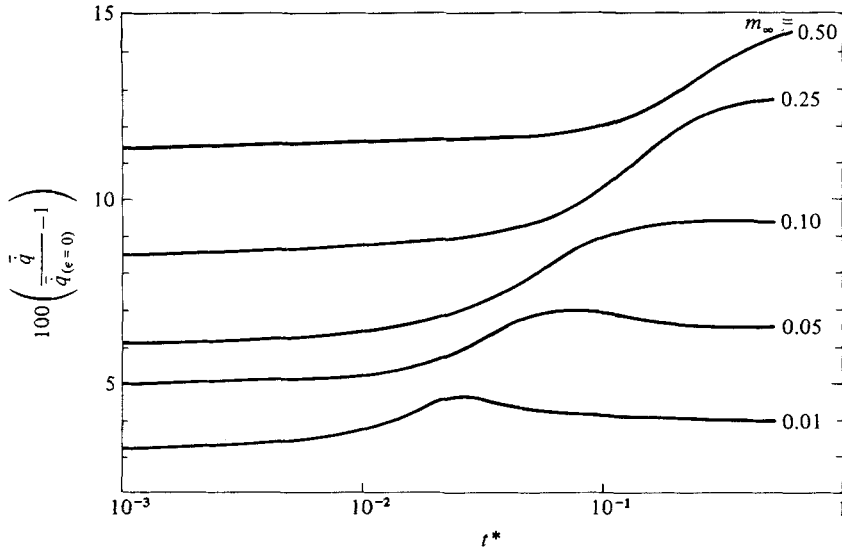
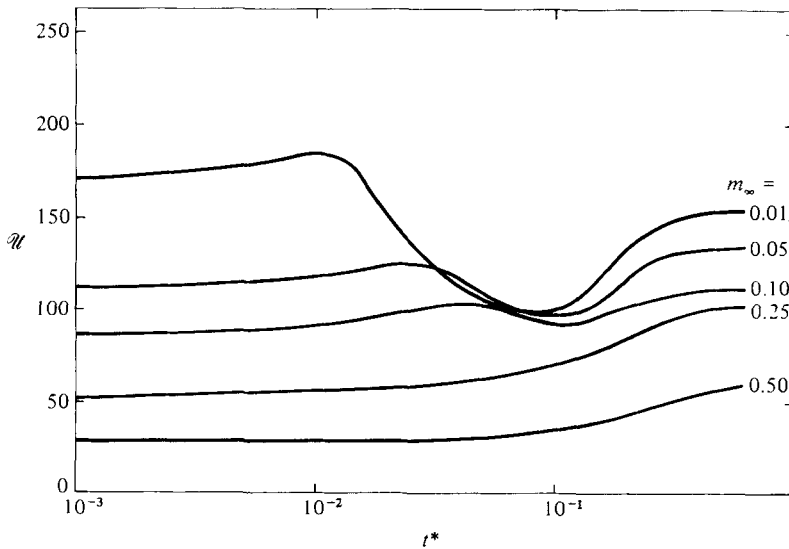FIGURE 5. The effect of drop translation on heat transfer; $T_0 = 30$ °C, $T_\infty = 100$ °C, $Re_{nc} = 0.5$.

FIGURE 6. The variation of overall conductance, $\mathcal{U}$ with dimensionless time; $T_0 = 30$ °C, $T_\infty = 100$ °C, $Re_{nc} = 0.5$.

at a much later t^*. However, this last statement has to remain a conjecture at this point.

The variation in the dimensionless overall conductance $\mathcal{U}$ is shown in figure 6. Very high conductances are realized during the early stages of motion because of the rather thin thermal boundary layer inside the drop. Large thermal gradients are possible due to the thinness of the thermal layer. With increasing time, the thermal boundary layer becomes thicker owing to transient diffusion of heat across the streamlines in the drop interior. This in turn causes the overall conductance to decrease because of a lesser temperature gradient. At a much later stage, the drop translational velocity
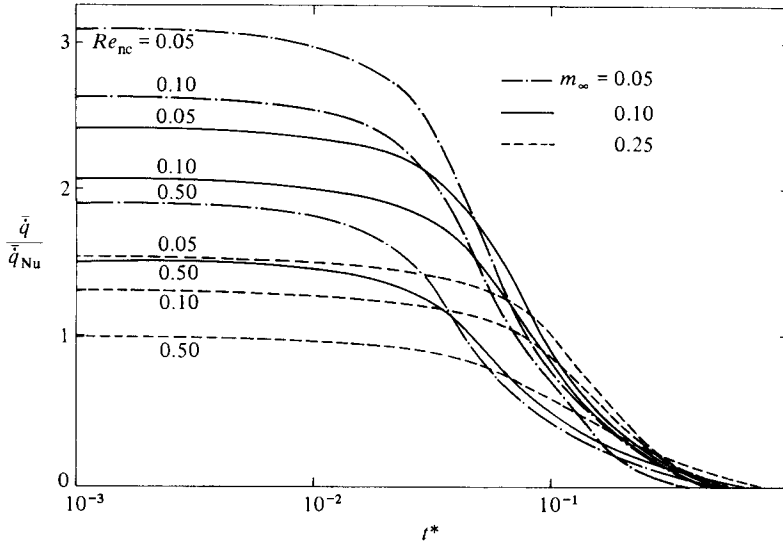
FIGURE 7. The effect of Reynolds number of flow on dimensionless heat transfer; $T_0 = 30$ °C, $T_\infty = 100$ °C.
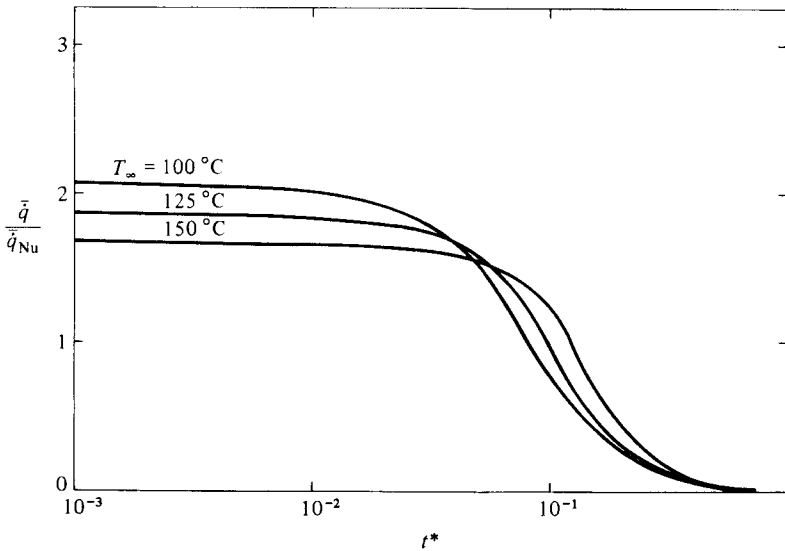

FIGURE 8. The effect of freestream temperature on dimensionless heat transfer; $T_0 = 30$ °C, $Re_{nc} = 0.1$, $m_\infty = 0.1$.

has increased significantly and there is vigorous internal circulation. Increased mixing results in a higher overall conductance. This explains the increasing characteristic.

Figure 7 presents the effects of Reynolds number Re_{nc} on dimensionless heat transfer. The ambient temperature is 100 °C and the non-condensable mass fractions are 0.05, 0.1 and 0.25. The Reynolds numbers studied are 0.05, 0.1 and 0.5. For small times $\bar{q}/\bar{q}_{Nu}$ is seen to vary inversely as the Reynolds number at a given m_∞. To understand this, we recall that $Re_{nc} \equiv f(U_\infty, R)$ for given ν. For a freely falling liquid drop, the terminal velocity $U_{\infty 0} \propto R^2$. Thus higher Reynolds numbers correspond
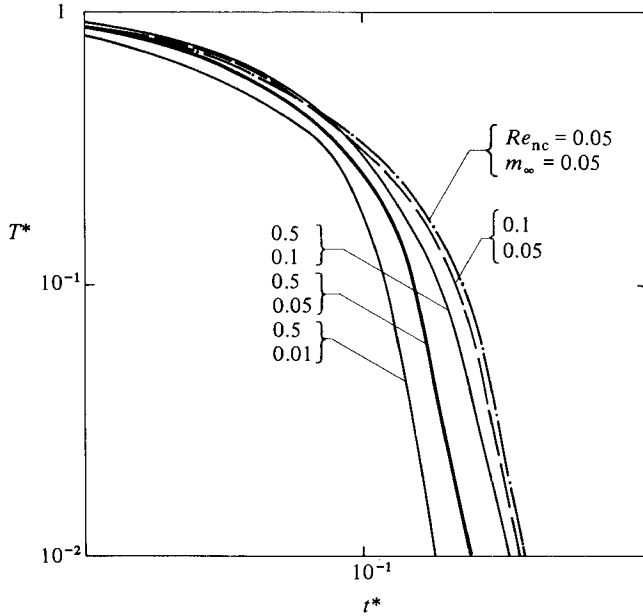
FIGURE 9. Mixing-cup temperature of the drop versus dimensionless time;
$T_0 = 30 \ ^\circ\text{C}$, $T_\infty = 100 \ ^\circ\text{C}$.

to both higher terminal velocities and droplet radii. The surface-area increase is such as to cause a reduction in the heat flux. For large times, however, the smaller drops (smaller Re) which experience higher heat-transfer rates during the initial stages show a higher rate of decrease in heat transport. This is due to the relatively smaller heat capacity and a tendency to thermally equilibrate faster. From an order-of-magnitude estimate, it can be shown that the condensation heat-transfer rate is expressible as follows for higher condensation rates:

$$\frac{\bar{\bar{q}}}{\bar{q}_{\text{Nu}}} = \left(\frac{\bar{\bar{q}}}{\bar{q}_{\text{Nu}}}\right)_0 + \epsilon\left(\frac{\bar{\bar{q}}}{\bar{q}_{\text{Nu}}}\right)_1, \tag{122}$$

where

$$\left(\frac{\bar{\bar{q}}}{\bar{q}_{\text{Nu}}}\right)_0 \propto R^{-\frac{3}{4}}, \quad \epsilon\left(\frac{\bar{\bar{q}}}{\bar{q}_{\text{Nu}}}\right)_1 \propto \frac{U_\infty}{R^{-\frac{1}{4}}}. \tag{123}$$

The size of the drop controls the heat transfer to all orders, while the forced flow field has influence only past the lowest order.

Figure 8 shows the variation of dimensionless heat transfer with freestream temperature T_∞. Three different prescribed ambient temperatures (100 °C, 125 °C and 150 °C) are analysed and droplet initial temperature is fixed at 30 °C for all the cases. The role played by the ambient temperature conditions can be appreciated by examining the results as appropriate to small times. $\bar{q}/\bar{q}_{\text{Nu}}$ decreases with increasing T_∞. This effect is similar to that found in high-Reynolds-number condensation heat transfer to a translating droplet (Chung & Ayyaswamy 1981). The terminal velocity (120) of a moving drop is strongly dependent on the prevailing thermodynamic conditions. The flow field is seriously affected by the ambient temperature. With increasing ambient temperature, the terminal velocity (freestream velocity) decreases. The resultant condensation flow field is weakened and the dimensionless heat transport is decreased. The decrease in dimensionless heat transfer is also due to $\bar{q}_{\text{Nu}}$ varying as $(T_\infty - T_i)^{\frac{1}{4}}$, while $\bar{q}$ does not increase as much. Although increased ambient
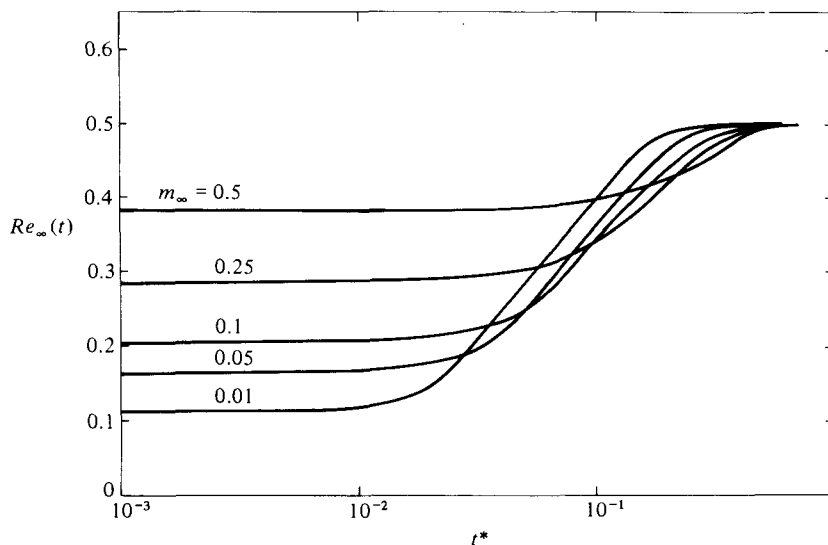
FIGURE 10. The variation of instantaneous Reynolds number with dimensionless time; $Re_{nc} = 0.5$. $T_0 = 30$ °C, $T_\infty = 100$ °C.

temperature provides increased thermal driving force, the two features discussed above seem to dominate.

Figure 9 is a plot of the mixing-cup temperature of the droplet versus time. We note that the decrease in the non-dimensional temperature observed in the figure corresponds to an actual increase of the drop temperature. This is because of the way the temperature has been non-dimensionalized, viz $T^* = (T_\infty - T)/(T_\infty - T_0)$. The average temperature of the drop increases with increasing time, independently of the Reynolds number and the non-condensable mass fraction. This is as would be expected. However, the rate at which this increase occurs depends on Re_{nc} and m_∞. Initially, a rapid increase in the average temperature occurs because of the low surface temperature following introduction. The internal circulation pattern during this initial period is such as to bring the colder water from the drop centre region to the outer surface. A high condensation rate is achieved. With increasing time, the centre temperature approaches the surface value, and the surface heat transfer becomes weaker. The vortex streamlines tend to become isothermal loops. Subsequent heat transfer occurs primarily in directions normal to vortex lines, with diffusion as the dominant mechanism. This explains the similarity of the slopes of the temperature–time characteristics after an initial period dominated by internal circulation.

The variation of the instantaneous Reynolds number $Re_\infty(t)$ for the drop as a function of dimensionless time is shown in figure 10. The representative Reynolds number Re_{nc} is 0.5. During the early stages of translation $Re_\infty(t)$ is less than Re_{nc}. This is due to the high drag experienced by the drop as a result of the strong radial field induced by condensation. With increasing time, the condensation flow field weakens and the translation velocity increases. Eventually, as the drop reaches thermal equilibrium with its ambient environment, the Reynolds number $Re_\infty(t)$ approaches the limiting value Re_{nc}. This figure clearly illustrates the effect of condensation on drop translation.

REFERENCES

ACRIVOS, A. & TAYLOR, T. D. 1962 Heat and mass transfer from single spheres in Stokes flow. *Phys. Fluids* **5**, 387–394.

CHUNG, J. N. & AYYASWAMY, P. S. 1981*a* Laminar condensation heat and mass transfer to a moving drop. *AIChE J.* **27**, 372–377.

CHUNG, J. N. & AYYASWAMY, P. S. 1981*b* Material removal associated with condensation on a droplet in motion. *Intl J. Multiphase Flow* **7**, 329–342.

CHUNG, J. N., AYYASWAMY, P. S. & SADHAL, S. S. 1984 Laminar condensation on a moving drop. Part 2. Numerical solutions. *J. Fluid Mech.* **139**, 131–144.

CLIFT, R., GRACE, J. R. & WEBER, M. E. 1978 *Bubbles, Drops and Particles.* Academic.

DENNIS, S. C. R., WALKER, J. D. A. & HUDSON, J. D. 1973 Heat transfer from a sphere at low Reynolds numbers. *J. Fluid Mech.* **60**, 273–283.

FENDELL, F. E., SPRANKLE, M. L. & DODSON, D. S. 1966 Thin-flame theory for a fuel droplet in slow viscous flow. *J. Fluid Mech.* **26**, 267–280.

SADHAL, S. S. & AYYASWAMY, P. S. 1983 Flow past a liquid drop with a large non-uniform radial velocity. *J. Fluid Mech.* **133**, 65–81.

YANG, J. W. 1973 Laminar film condensation on a sphere. *Trans. ASME* C: *J. Heat Transfer* **95**, 174–178.